

Ga/N flux ratio influence on Mn incorporation, surface morphology, and lattice polarity during radio frequency molecular beam epitaxy of (Ga,Mn)N

Muhammad B. Haider, Costel Constantin, Hamad Al-Brithen, Haiqiang Yang, Eugen Trifan, David Ingram, and Arthur R. Smith^{a)}

Condensed Matter and Surface Science Program, Department of Physics and Astronomy, Ohio University, Athens, Ohio 45701

C. V. Kelly and Y. Ijiri

Department of Physics and Astronomy, Oberlin College, Oberlin, Ohio 44074

(Received 25 September 2002; accepted 13 February 2003)

The effect of the Ga/N flux ratio on the Mn incorporation, surface morphology, and lattice polarity during growth by rf molecular beam epitaxy of (Ga,Mn)N at a sample temperature of 550 °C is presented. Three regimes of growth, N-rich, metal-rich, and Ga-rich, are clearly distinguished by reflection high-energy electron diffraction and atomic force microscopy. Using energy dispersive x-ray spectroscopy, it is found that Mn incorporation occurs only for N-rich and metal-rich conditions. For these conditions, although x-ray diffraction in third order does not reveal any significant peak splitting or broadening, Rutherford backscattering clearly shows that Mn is not only incorporated but also substitutional on the Ga sites. Hence, we conclude that a $\text{Mn}_x\text{Ga}_{1-x}\text{N}$ alloy is formed (in this case $x \sim 5\%$), but there is no observable change in the c -axis lattice constant. We also find that the surface morphology is dramatically improved when growth is just slightly metal rich. When growth is highly metal-rich, but not Ga-rich, we find that Ga polarity flips to N polarity. It is concluded that the optimal growth of Ga-polar MnGaN by rf N-plasma molecular beam epitaxy occurs in the slightly metal-rich regime. © 2003 American Institute of Physics.
[DOI: 10.1063/1.1565511]

I. INTRODUCTION

The formation of magnetic semiconductors is of widespread interest due to the possibility of making highly efficient spin injectors for spintronics applications. According to the prediction of Dietl *et al.*¹ ferromagnetic MnGaN is very promising since it should have a Curie temperature above room temperature (300 K). Therefore, the formation of a uniform MnGaN alloy is a crucial issue which needs to be explored.

There are many challenges to the formation of a uniform MnGaN alloy film. For example, Mn–N growth results in films in which Mn has octahedral bonds with N, whereas Ga prefers tetrahedral bonding.² In the case of alloy growth, it may also be relevant that the vapor pressure of Mn metal is about 100 times greater than that of Ga metal. Generally, the challenges combined with the great technological possibilities render the MnGaN system quite interesting to study, as is also evident by the appearance of several theoretical works.^{3–5}

Already, many experimental efforts have been reported regarding the preparation and magnetic properties of (Ga,Mn)N layers.^{6–8} There have been a number of reports on the use of molecular-beam epitaxy (MBE) to grow (Ga,Mn)N using either radio frequency (rf) plasma,^{6,9–11} electron-cyclotron-resonance (ECR) plasma,¹² or ammonia¹³ for the nitrogen source. Despite many promising results, the

reported growth conditions, as revealed by reflection high-energy electron diffraction (RHEED), appear to vary widely. For example, Kuwabara *et al.*⁶ who used rf N-plasma, showed a streaky RHEED pattern and reported Mn incorporation as high as 11% without macroscopic precipitation for a substrate temperature of 600 °C. On the other hand, Overberg *et al.*¹⁰ who also used rf N-plasma reported a partially spotty RHEED pattern and a Mn concentration of 7.0 at. %. Sonoda *et al.*,¹³ who used ammonia, reported a sample which was apparently grown with a streaky RHEED pattern and without precipitation. Yet, Cui and Li¹² reported that ECR MBE using a nitrogen–hydrogen plasma resulted in a spotty RHEED pattern and a $\text{Mn}_x\text{Ga}_{1-x}\text{N}$ alloy without precipitation. Thus, while it is therefore unclear whether streaky or spotty RHEED patterns are preferable for incorporation, it is well known that a spotty RHEED pattern implies rough three-dimensional (3D) growth whereas a streaky RHEED pattern, implying smooth two-dimensional growth, is much more desirable from the point of view of forming smooth interfaces for heterostructures. In addition, few reports have mentioned lattice constant changes for MnGaN with respect to GaN, except for those cases involving growth in the presence of hydrogen.^{12,14} Thus, it is also unclear whether growth with hydrogen is necessary for incorporation on substitutional sites.

Therefore, it is important to investigate the growth conditions without hydrogen which may result in both Mn incorporation *and* smooth surface morphology *and* to provide compelling evidence that the Mn incorporation is occurring on Ga sites. To achieve these goals requires systematic in-

^{a)} Author to whom correspondence should be addressed; electronic mail: smitha2@ohio.edu

vestigations of the effects of various growth conditions on the film properties. One of the most important variables in the growth of $\text{Mn}_x\text{Ga}_{1-x}\text{N}$ is the Ga/N flux ratio. Here, we present a study of the effects of the Ga/N flux ratio on the aforementioned properties using rf N-plasma MBE. It will be shown that this parameter is critical in determining both incorporation and film morphology, and the growth condition will be shown which can optimize these two properties. In addition, it is also shown that the Ga/N flux ratio affects the resulting film polarity. The results are explained in terms of three separate regimes of growth, each corresponding to a certain type of surface structure.

II. EXPERIMENT

The growth experiments are performed in a custom MBE system utilizing gallium and manganese effusion cells and a rf-plasma source with N_2 as the source gas. The substrates are wurtzite Ga-polar GaN(0001) grown by metalorganic chemical vapor deposition (MOCVD) on sapphire and are either Si-doped *n* type at $1-3 \times 10^{18} \text{ cm}^{-3}$ or unintentionally doped *n* type at $5 \times 10^{16}-5 \times 10^{17} \text{ cm}^{-3}$. The substrates are loaded into the MBE chamber and heated up to 550°C which is maintained throughout the entire growth. The N-plasma source is applied using 500 W with a N_2 flow rate of 1.1 standard cubic centimeters per minute. The chamber background pressure = 9×10^{-6} Torr. The Ga and Mn fluxes, J_{Ga} and J_{Mn} , are measured by a crystal thickness monitor held at room temperature. The Ga/N flux ratio ($J_{\text{Ga}}/J_{\text{N}}$) is set in the range from 0.7 (N-rich) to 1.46 (Ga-rich) with constant N flux. The Mn/N flux ratio ($J_{\text{Mn}}/J_{\text{N}}$) is set to ~ 0.07 . The growth begins with a 30 nm thick GaN buffer layer (no intentional doping), and then the Mn shutter is opened to grow the (Ga,Mn)N layer with thickness in the range 0.3–0.6 μm . Finally, a 30 nm thick GaN cap layer is grown.

The growth is monitored *in situ* by RHEED, and the films are studied *ex situ* by scanning electron microscopy (SEM), energy dispersive x-ray spectroscopy (EDX), x-ray diffraction (XRD), atomic force microscopy (AFM), rutherford backscattering (RBS), and vibrating sample magnetometry (VSM). The XRD machine uses Cu $K\alpha$ x rays, and the RBS uses an incident beam of 3.05 MeV He ions.

III. RESULTS AND DISCUSSION

A. Surface structure

In the case of binary GaN growth, there are two growth regimes—namely, N-rich and Ga-rich.^{15–17} The line between these two regimes is the point at which the net Ga flux is equal to the net N flux, and this line is easy to determine experimentally. For a dilute ternary alloy like (Ga,Mn)N, there are three growth regimes—namely, N-rich, metal-rich, and Ga-rich, as indicated by the growth map for (Ga,Mn)N shown in Fig. 1. We should expect that the (Ga,Mn)N film properties will be different in these three regimes as they are quite different for the two regimes of GaN growth.

Yet, it is not a simple matter to define these three conditions quantitatively based upon the measured Ga, Mn, and N fluxes since the surface sticking coefficients for these atoms

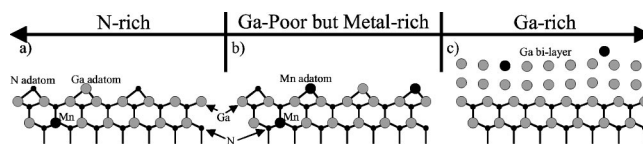


FIG. 1. Growth map for (Ga,Mn)N showing three growth regimes and the corresponding schematic surface structure models.

vary with surface structure. However, we find that these three regimes can be defined qualitatively as follows: (1) N-rich: Surface N atoms more than surface metal atoms; (2) metal-rich: Surface metal atoms (Ga plus Mn) more than surface N atoms; and (3) Ga-rich: surface Ga atoms more than surface N atoms. The ratio of the chemical species present on the surface (e.g., Ga/N) is a function of the Ga, Mn, and N fluxes, but it is certainly not directly equal to the ratio of those flux values. This is because the sticking coefficient S for each species varies as a function of the chemical potential of the surface, which in turn is a function of the flux ratios. And, the chemical potential of the surface in turn determines the surface structure which affects the growth mode. For example, under Ga-rich growth conditions in which the interaction is mainly between Ga and weakly bound Ga on the surface, S_{Ga} will be smaller than S_{Ga} under Ga-poor conditions in which there is not only a Ga–Ga interaction but also a stronger Ga–N interaction between the incident Ga and the surface. Thus, it is difficult to determine *a priori* where the lines should be drawn between these separate growth regimes just based on the flux ratios.

However, in the following, we shall describe the results in terms of the Ga/N flux ratio, which we define equal to unity at the metal-rich/Ga-rich transition point. We find this transition point to be identical, within uncertainty, to the transition point for binary GaN growth, for reasons to be explained later. Setting the Ga flux at this transition point equal to the N flux allows us to define the Mn/N flux ratio, and for this study, that has been held constant at $J_{\text{Mn}}/J_{\text{N}} = 0.07$.

Shown in Figs. 2(a)–2(e) are RHEED patterns during (Ga,Mn)N growth as a function of the Ga/N flux ratio as seen along $[11\bar{2}0]$. Results for the first sample are presented in Fig. 2(a) for $J_{\text{Ga}}/J_{\text{N}} = 0.76$ ($J_{\text{metal}}/J_{\text{N}} = 0.83$). The RHEED pattern is very spotty, indicating a 3D growth mode. For the case of $J_{\text{Ga}}/J_{\text{N}} = 0.84$ ($J_{\text{metal}}/J_{\text{N}} = 0.91$), as shown in Fig. 2(b), the pattern is much less spotty, indicating smoother growth. In Fig. 2(c) is the case for $J_{\text{Ga}}/J_{\text{N}} = 0.92$ ($J_{\text{metal}}/J_{\text{N}} = 0.99$), in which the RHEED pattern shows distinct nodes. Shown in Fig. 2(d) is the case for $J_{\text{Ga}}/J_{\text{N}} = 0.98$ ($J_{\text{metal}}/J_{\text{N}} = 1.05$) and, here, the RHEED pattern is more streaky. Finally, shown in Fig. 2(e) is the case for $J_{\text{Ga}}/J_{\text{N}} = 1.01$ ($J_{\text{metal}}/J_{\text{N}} = 1.08$). The RHEED pattern is very streaky, indicating a very smooth growth surface. This is also seen even at very high Ga/N flux ratios (e.g., $J_{\text{Ga}}/J_{\text{N}} = 1.46$). All of the RHEED patterns during growth are 1×1 without any fractional streaks. The samples of Figs. 2(a)–2(d) are all shiny with a slight tan color, whereas the sample of Fig. 2(e) has a hazy appearance.

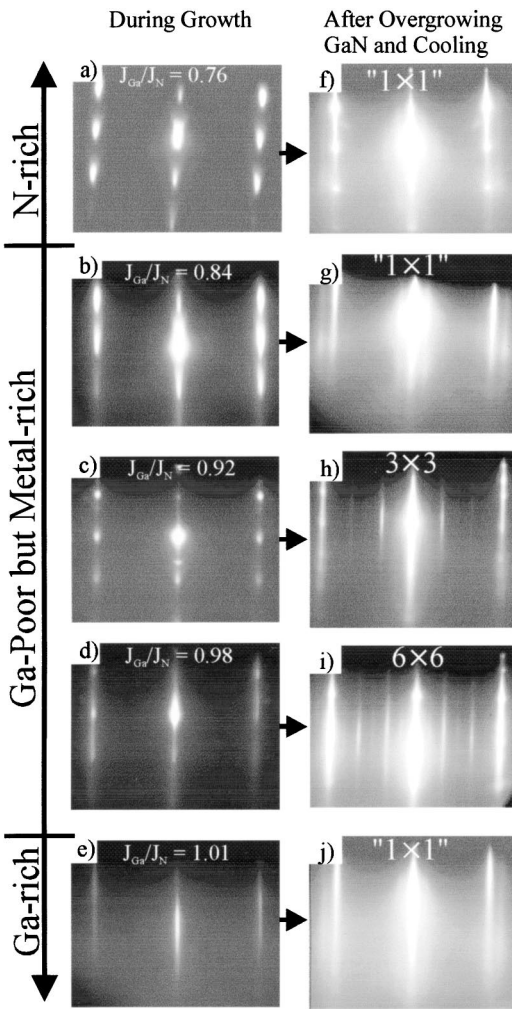


FIG. 2. (a–e) RHEED patterns during (Ga,Mn)N growth as a function of Ga/N flux ratio along $[11\bar{2}0]$; (f–j) RHEED patterns after Ga-rich GaN overgrowth and cooling to below 200 °C.

AFM images were acquired to measure the morphology of the films and to correlate with the RHEED patterns. In these AFM studies, special samples were grown under the same conditions but without the GaN cap layer so that the (Ga,Mn)N surface could be studied directly.

Shown in Fig. 3(a) is the AFM image of the (Ga,Mn)N film grown under the condition $J_{metal}/J_N=0.83$. The image in Fig. 3(a) shows a very rough surface, correlating well with the spotty RHEED pattern of Fig. 2(a). A zoom-in AFM image of the same surface is shown to the right-hand side. The surface consists of small hillocks of about 0.25 μm in lateral dimension, and these are spaced closely together. The root-mean-square (rms) surface roughness is 81 Å with a peak-to-valley height of 685 Å. Thus, a 3D growth mode is observed. We find that this surface is consistent with growth under N-rich conditions.

Rough 3D growth is well known to occur under N-rich conditions in the case of GaN grown by rf N-plasma MBE.^{15–17} Here, we find that the Mn atoms make little difference in this behavior, and a schematic model of the surface during growth is shown in Fig. 1(a). Under N-rich conditions, it is understood that the N accumulates on the GaN

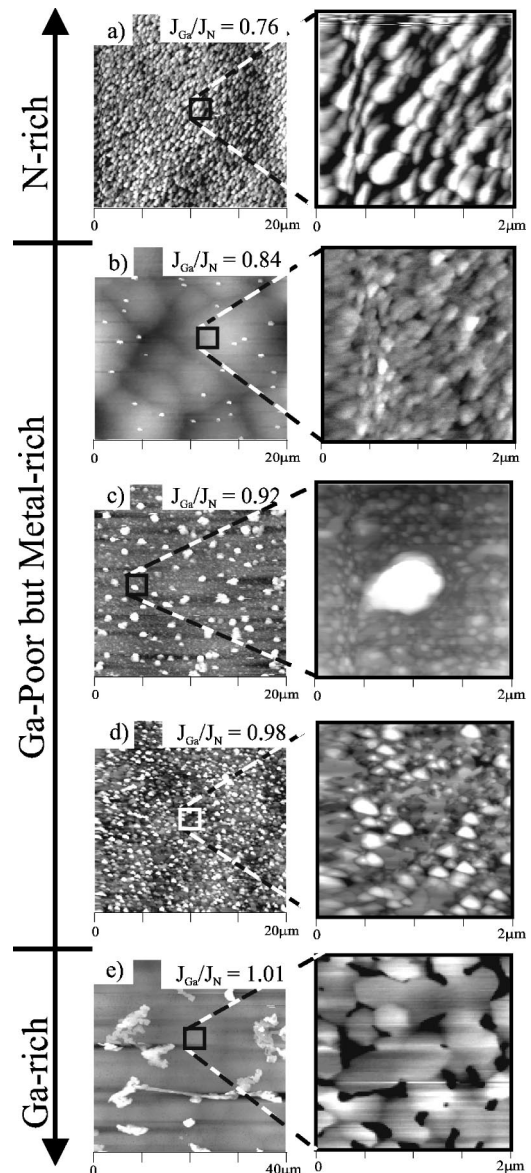


FIG. 3. AFM images following (Ga,Mn)N growth as a function of Ga/N flux ratio.

surface, resulting in a dramatically reduced surface diffusion for both Ga and N atoms.¹⁸ The diffusion barrier for Mn atoms on such a N-rich surface is expected to be similarly high. This will prevent Mn from accumulating in precipitates, but will result in a rough 3D growth.

Shown in Fig. 3(b) is the AFM image of the film surface for $J_{metal}/J_N=0.91$ together with a zoom in. In contrast to the surface of Fig. 3(a), this surface is clearly smoother, correlating well with the RHEED pattern of Fig. 2(b). The rms surface roughness of the zoom-in region is ~ 12 Å, substantially less than for N-rich growth. Such a strikingly smoother growth morphology indicates a major change in the growth mode; thus, we conclude that this sample was not grown in N-rich conditions but rather in slightly metal-rich conditions.

The smoothening behavior for this sample suggests that the surface diffusion is substantially increased compared to N-rich conditions. This could well be explained as being due to the effect of the excess surface metal, as indicated sche-

matically in the surface model shown in Fig. 1(b). Since metal atoms are dominant on the surface, N atoms are prevented from accumulating on the surface. This results in larger surface diffusion length, and the surface is smoother compared to N-rich growth.

Further evidence that the surface is metal rich is given by the appearance of tiny dots, as seen in the AFM image of Fig. 3(b). Their lateral dimension is about $0.5 \mu\text{m}$ with height of $0.01\text{--}0.03 \mu\text{m}$, and there are $\sim 0.1 \text{ dots } \mu\text{m}^{-2}$. Since such dots are not observed for the case of binary GaN growth, they are evidently caused by the Mn at the surface. The excess metal which is not used up eventually forms metallic precipitates. We emphasize that the metal-rich conditions refer to the surface and is therefore a function of the atom sticking coefficients as well as the flux ratio, which is why a metal/N flux ratio of 0.91 is entirely consistent with metal-rich conditions. The lack of any other good explanation for the growth mode transition we observe near $J_{\text{metal}}/J_{\text{N}}=0.91$ further supports our conclusion.

Shown in Fig. 3(c) are AFM images of the surface grown with $J_{\text{metal}}/J_{\text{N}}=0.99$. Clearly, we observe an increased density of the tiny dots on the surface. This increased density is attributed to the increased metal-rich surface conditions. The dots themselves have lateral dimension of about $1 \mu\text{m}$ with a height of about $0.1\text{--}0.2 \mu\text{m}$, and we observe $\sim 0.3 \text{ dots } \mu\text{m}^{-2}$. The areas between the tiny dots are somewhat rougher in comparison to Fig. 3(b), having a rms roughness of $\sim 90 \text{ \AA}$. This rough surface correlates well with the RHEED pattern of Fig. 2(c).

Shown in Fig. 3(d) are AFM images of the (Ga,Mn)N film grown with $J_{\text{metal}}/J_{\text{N}}=1.05$. Here, we observe a further increase of the dotlike features. They have typical lateral dimension of $\sim 0.25 \mu\text{m}$ with a height of $0.05\text{--}0.1 \mu\text{m}$ and a density of $\sim 7 \text{ dots } \mu\text{m}^{-2}$. Therefore, about 33% of the total surface area is covered by the dots. However, some areas between the dots appear somewhat smooth, which agrees well with the fairly streaky RHEED pattern of Fig. 2(d).

Thus, over the range of metal-rich conditions we find clear evidence for tiny dotlike precipitates which increase in density as the conditions become more metal rich. As conditions become closer to N-rich, the size of the dot decreases. These tiny dots do not significantly affect the RHEED pattern, probably because they have a random crystalline alignment with the substrate. We also find that when the density of the dots becomes small (going toward N-rich conditions), the surface shows much improved smoothness. This implies that the less excess metal there is on the surface, the better the surface morphology. Beyond this, when the conditions become N rich, the dots no longer appear since there is no excess surface metal, N atoms accumulate on the surface,¹⁸ and 3D growth occurs.

Shown in Fig. 3(e) is the AFM image for a sample grown with $J_{\text{Ga}}/J_{\text{N}}=1.01$ ($J_{\text{metal}}/J_{\text{N}}=1.08$) and the zoom in image of that surface. This image clearly reveals a qualitatively different type of surface morphology characterized by very smooth areas and some large precipitates. These precipitates have irregular shapes, some being more compact and some having a linear shape. The compact ones have lateral dimensions ranging from $2\text{--}10 \mu\text{m}$, heights varying

from $0.1\text{--}0.9 \mu\text{m}$, and we see $\sim 5 \times 10^{-3} \mu\text{m}^{-2}$. The linear islands can be very long; in some SEM images, they go on for several hundred μm or more.

The zoom in image of the smooth area between the large precipitates shows the typical morphology of a smooth GaN surface grown under Ga-rich conditions by rf MBE.¹⁷ A further zoom in (not shown) of this smooth surface reveals individual atomic-height steps.

The precipitates contain large amounts of Mn as revealed by EDX (see next). To understand why the Ga-rich conditions lead to large Mn precipitation with atomically smooth regions in between the precipitates, it is useful to consider the structure of the GaN surface under Ga-rich conditions. As has been previously reported in several different places, it is now well understood that the Ga-rich surface of Ga-polar GaN consists of a liquid Ga bilayer.^{17,19,20} This liquid layer of Ga metal at the growth temperature is like a "sea" of atoms all moving rapidly. Based on the strong similarity of the growth behavior in Ga-rich conditions for (Ga,Mn)N and GaN, we conclude that the surface structure is nearly the same for the two cases. For (Ga,Mn)N, Mn dopants added to this liquid Ga bilayer are evidently not able to penetrate it. This is reasonable considering the high-energetic stability of the Ga bilayer and the fact that the vapor pressure of Mn is of the order of 10^2 larger than Ga at the growth temperature. So instead, the Mn dopants are carried along on top of the layer or within the top monolayer.

The schematic picture of the surface during growth is shown in Fig. 1(c). Since most likely it is the lower monolayer of Ga atoms which mainly participates in GaN growth (at step edges for example), the Mn atoms are never able to come into contact with the top-most GaN bilayer (growth sites). Thus, the Mn is not incorporated. The Mn atoms are carried along the surface until Mn-rich islands begin to form. The liquid Ga sea continues to bring Mn to these islands and they grow, resulting in the observed precipitates seen in Fig. 3(e). The linear features in Fig. 3(e) are presumably caused by the anisotropic growth of the Mn-containing islands. The tallest islands also correspond to the ones having smaller lateral dimensions. Finally, the fact that Mn atoms are evidently swept away by the Ga bilayer is also the explanation for why the Ga-rich transition point is changed little compared to growth without Mn.

B. Effect of flux ratio on film polarity

Now, we address the issue of the film polarity. RHEED patterns have been shown to be identifiers of the polarity of GaN by Smith *et al.*²¹ To verify the polarity of our (Ga,Mn)N films, they were overgrown with GaN and then cooled to less than 200°C . It is known that if the film has Ga polarity, a pseudo- 1×1 (" 1×1 ") pattern will be observed at low temperatures. On the other hand, if a 3×3 or 6×6 pattern emerges, then the film has N polarity.

As shown in Fig. 2(f) for the N-rich grown (Ga,Mn)N film, the pattern after overgrowing and cooling clearly shows the 1×1 with faint outside additional streaks, the characteristic of the " 1×1 " surface, thus showing the Ga polarity of the substrate was maintained.²¹ Similarly, we observe the

"1×1" pattern for the case of slightly metal-rich growth, as shown in Fig. 2(g), again proving the Ga polarity of the substrate is maintained for the film.

When the conditions of growth become more metal-rich, however, we observe a different result. Namely, after cooling the Ga-rich overgrown layer, the RHEED pattern shows both 3×3 and 6×6 structure, as shown in Figs. 2(h) and 2(i), respectively. This indicates that the polarity of the (Ga,Mn)N film, grown on a Ga-polar GaN substrate, has apparently flipped to become N polar.²¹

Finally, the result of the polarity test for the case of Ga-rich growth of (Ga,Mn)N is displayed in Fig. 2(j). Clearly, upon cooling, the RHEED pattern shows the characteristics of the "1×1" with no sign of 3×3 or 6×6. Thus, the (Ga,Mn)N film grown under Ga-rich conditions remains Ga polar.

Based on our previous discussions of the surface structure during growth for the three different regimes, the polarity dependence can be understood as follows. Under N-rich or slightly metal-rich conditions, Mn atoms at the surface do not build up much higher concentration than in the bulk (~5%). They are thus incorporated and do not modify the polarity. Under Ga-rich conditions, the Mn atoms are swept away by the liquid Ga bilayer and also cannot modify the Ga polarity. However, under substantially metal-rich conditions (but not Ga-rich), it may be that excess Mn accumulates at the surface, forming a Mn-rich surface layer. It has been reported that a magnesium-rich surface layer causes polarity flipping from Ga to N polar.²² Thus, we infer that a similar mechanism occurs for the case of manganese.

C. Bulk structure and chemical content

The samples were analyzed using SEM, and EDX spectra were collected to assess the chemical content. Shown in Fig. 4(a) is the EDX spectrum of the N-rich grown sample ($J_{\text{Ga}}/J_{\text{N}}=0.76$) corresponding to Figs. 2(a) and 3(a). The Ga $K\alpha_1$ and Ga $K\alpha_2$ peaks are evident, and also small Mn $K\alpha_1$ and Mn $K\alpha_2$ peaks are seen. The Mn/Ga peak area ratio is about 4.3%, which also samples the Ga of the GaN substrate. As the AFM image of this sample [Fig. 3(a)] indicates a homogeneous layer without any precipitates, we infer that the Mn is incorporated uniformly in the layer.

Shown in Fig. 4(b) is the EDX spectrum of the metal-rich grown sample ($J_{\text{metal}}/J_{\text{N}}=1.05$) corresponding to Figs. 2(d) and 3(d). Both Mn and Ga peaks are observed, and the Mn/Ga peak area ratio is similar to that of the N-rich grown sample. The AFM image of Fig. 3(d) indicates a homogeneous surface at a large scale but some inhomogeneities at a smaller scale. However, the EDX spectrum averages over these small features and, therefore, it only suggests the Mn is possibly incorporated in the layer for this metal-rich condition.

Shown in Fig. 4(c) are EDX spectra for a Ga-rich grown sample ($J_{\text{Ga}}/J_{\text{N}}=1.21$) with a surface similar to that shown in Fig. 3(e). These spectra were acquired with the electron beam focused on particular regions. The lower spectrum is representative of the compact precipitates seen in the AFM image. It shows Mn peaks which are almost half as large as

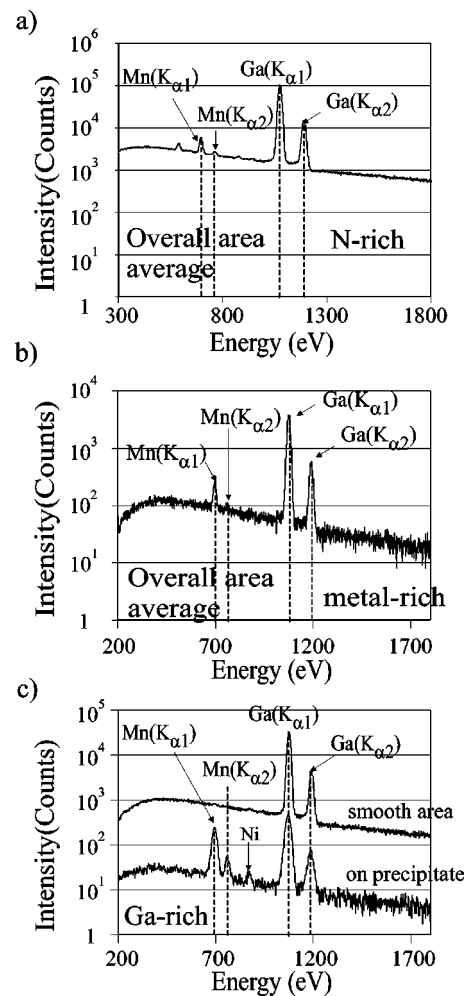


FIG. 4. EDX spectra as a function of the Ga/N flux ratio: (a) N-rich ($J_{\text{Ga}}/J_{\text{N}}=0.76$), (b) metal-rich ($J_{\text{Ga}}/J_{\text{N}}=0.92$), and (c) Ga-rich ($J_{\text{Ga}}/J_{\text{N}}=1.21$). For (c), upper spectrum is for the region between the precipitates; lower spectrum is for one of the compact-shaped precipitates, showing a Mn/Ga peak area ratio of 43%.

the Ga peaks, and the Mn/Ga peak area ratio is ~43% (Note: The Ga signal may also partly come from the GaN substrate). Thus, the Mn content of these precipitates is quite large. Also, for the linear features, we observe a large Mn/Ga peak area ratio of ~18% (spectrum not shown). The upper spectrum is representative of the smooth areas in between the precipitates. These areas have a quite different chemical content—the EDX spectrum shows no sign of Mn peaks. Therefore, these regions have little if any Mn. Thus, for Ga-rich growth conditions, the resulting film has a highly non-uniform Mn incorporation. Indeed, it appears that most of the film is mainly GaN with the Mn precipitating into concentrated clumps and linear features. This is consistent with what Cui and Li¹² observed for their growth without adding hydrogen. The crystalline structure of these microscopic precipitates has not been determined.

To provide an additional independent measurement regarding Mn incorporation, RBS was performed on the films. Results for the N-rich, metal-rich, and Ga-rich (Ga,Mn)N films are shown in Figs. 5(a), 5(b), and 5(c), respectively.

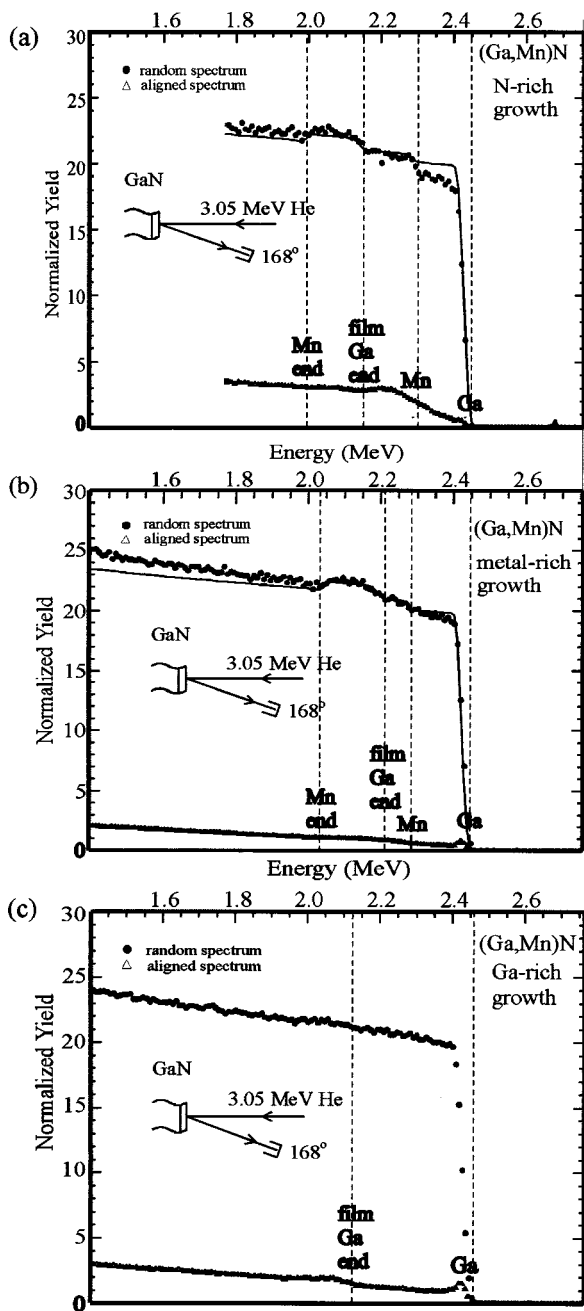


FIG. 5. RBS spectra as a function of Ga/N flux ratio: (a) N-rich ($J_{Ga}/J_N = 0.76$), (b) metal-rich ($J_{Ga}/J_N = 0.92$), and (c) Ga-rich ($J_{Ga}/J_N = 1.21$). Dark dotted data points represent the randomly aligned data; light triangle points represent the aligned data (crystal axis aligned with He ion beam). The continuous black curves represent simulations using the RUMP code.

For N-rich growth, Fig. 5(a) shows the random (incident beam randomly aligned with sample normal) spectrum (dark dots), clearly revealing the presence of a Mn hump at an energy of ~ 2.28 MeV. The data agree well with the Rutherford universal manipulation program (RUMP) simulated spectrum (black line) for a layer having $\sim 5\%$ Mn/Ga.²³ The smaller data values compared to the model fit near the Ga onset (surface region) are due to the surface roughness shown in Fig. 3(a) not taken into account in the model. The aligned spectrum (light triangles) shows a rapidly rising signal, indicating poor channeling for the film, followed by a

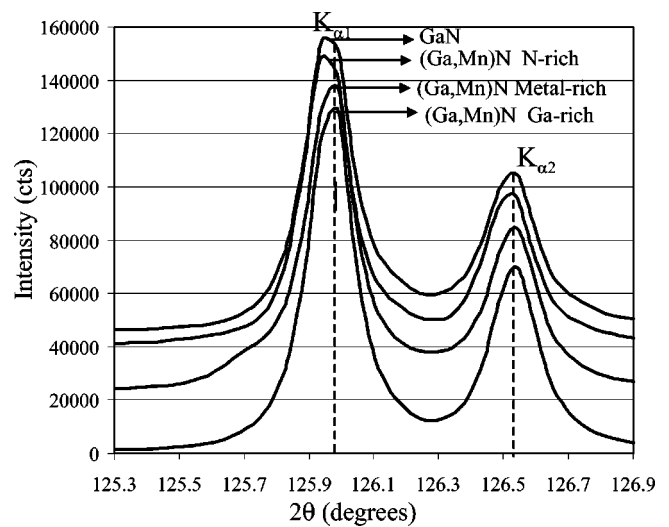


FIG. 6. XRD 2θ spectra near 126° for MBE-grown GaN (control sample), N-rich grown (Ga,Mn)N, metal-rich grown (Ga,Mn)N, and Ga-rich grown (Ga,Mn)N, showing the 0006 GaN peak region. Vertical offsets have been added for clarity.

more slowly rising part, indicating good channeling for the substrate. A likely cause of the poor film channeling could be the presence of interstitial metal atoms; we also observed similar behavior for MBE-grown GaN under N-rich conditions.

For the case of metal-rich growth [Fig. 5(b)], the presence of Mn is also revealed by the Mn onset at energy ~ 2.28 MeV in the random spectrum (dark dots). The data agree well with the RUMP simulated spectrum (black line) for a layer having $\sim 5\%$ Mn/Ga. In addition, the aligned spectrum (light triangles) in Fig. 5(b) shows a slowly rising signal, indicating good film channeling and no clear Mn hump. This suggests that the Mn atoms in the film are well aligned with the Ga atoms and that there are negligible interstitial atoms. This is strong evidence that the incorporated Mn is substitutional on the Ga sites. Thus, the slightly metal-rich growth regime has the attributes of a comparably smooth surface [indicated by the AFM image of Fig. 3(b)] as well as Mn incorporation and is thus a candidate for the ideal conditions for growing the highest-quality MnGaN layers using rf N-plasma MBE.

For Ga-rich growth, the random (dark dots) spectrum in Fig. 5(c) indicates the presence of Ga only in the film, and there is no indication of any Mn signal. The aligned spectrum (light triangles) shows an interface between the film and MOCVD GaN at energy 2.1 MeV and also no evidence for any Mn. Although the EDX clearly reveals Mn on the surface in the form of precipitates, the RBS is sensitive to the total volume fraction of Mn, which is apparently very small.

The crystallinity of the layers was assessed using XRD. Shown in Fig. 6 are the XRD results for four films: (1) MBE-grown GaN on MOCVD GaN substrate (control sample in N-rich conditions, $J_{Ga}/J_N = 0.7$), (2) (Ga,Mn)N under N-rich conditions ($J_{Ga}/J_N = 0.76$), (3) (Ga,Mn)N under metal-rich conditions ($J_{Ga}/J_N = 0.92$), and (4) (Ga,Mn)N under Ga-rich conditions ($J_{Ga}/J_N = 1.21$). Shown is the third-order 0006 peak region for GaN near $2\theta = 126^\circ$. Both the $K\alpha_1$ and the

$K\alpha_2$ peaks are clearly resolved for all four films at 125.96° and 126.53° , respectively. Given that $\lambda(\text{Cu } K\alpha_1)=1.540 \text{ \AA}$ and $\lambda(\text{Cu } K\alpha_2)=1.544 \text{ \AA}$, the known lattice constant of GaN, $c=5.186 \text{ \AA}$, is obtained.²⁴

Surprisingly, the positions of the peaks are the same for all four films to within 0.005° , implying a lattice constant change of $<0.0001 \text{ \AA}$ with respect to c of GaN. We also find little evidence for broadening of the 0006 peak for the three (Ga,Mn)N films.

Only Cui and Li¹² and Sonoda *et al.*¹⁴ reported lattice constant shifts for their GaMnN samples grown using N_2H_2 plasma and ammonia, respectively. In fact, we note that Cui and Li¹² reported an increase in the c -axis lattice constant while Sonoda *et al.*¹⁴ reported a decrease in the c -axis lattice constant.

Our observations are consistent with many other papers not reporting peak shifts for MnGaN samples grown using rf N-plasma MBE.^{6,9-11} And, our EDX and RBS results clearly show the incorporation of $\sim 5\%$ Mn in our N-rich and metal-rich grown films. Thus, we can only conclude that the bilayer spacing in wurtzite GaN is not very much affected by such small Mn concentrations.

D. Magnetic properties

Lastly, we compare the magnetic properties of the films using VSM. The magnetic measurements have been done at room temperature and are shown in Figs. 7(a)–7(c).

The VSM measurement of the N-rich grown sample ($J_{\text{Ga}}/J_{\text{N}}=0.76$) is shown in Fig. 7(a). After subtraction of the diamagnetic contribution from the sapphire substrate, the film shows a weak diamagnetic behavior with little indication of ferromagnetic (FM) behavior.

The VSM measurement of the metal-rich grown sample ($J_{\text{Ga}}/J_{\text{N}}=0.92$) is shown in Fig. 7(b). Again, only a weak diamagnetic behavior is observed with little sign of FM behavior. However, we do note that both the N-rich and metal-rich grown films show a tiny separation in their hysteresis loops.

There are several probable explanations for the negligible FM behavior for N-rich and metal-rich growth. One reason could be that VSM lacks the sufficient sensitivity to observe it. A second possible explanation is that the sample needs to have the correct carrier type and concentration, whereas we have not yet attempted to specifically dope the film. The Mn may act as an acceptor in a film which would otherwise be n type due to small concentrations of N vacancies or other unintentional impurities. Thus, the film could even be insulating. A third possibility is that the Mn concentration needs to be higher or lower, as indicated by a recent theory paper.²⁵ Future studies will need to focus on the effects of Mn concentration and intentional doping.

The VSM result for the Ga-rich grown sample ($J_{\text{Ga}}/J_{\text{N}}=1.21$) is shown in Fig. 7(c). After subtracting the diamagnetic contribution from the sapphire substrate, a small FM loop is observed. This small FM behavior cannot however be attributed to the (Ga,Mn)N since the previously discussed RBS and EDX results show that very little Mn is incorporated into the GaN in the Ga-rich growth case. Ga-rich

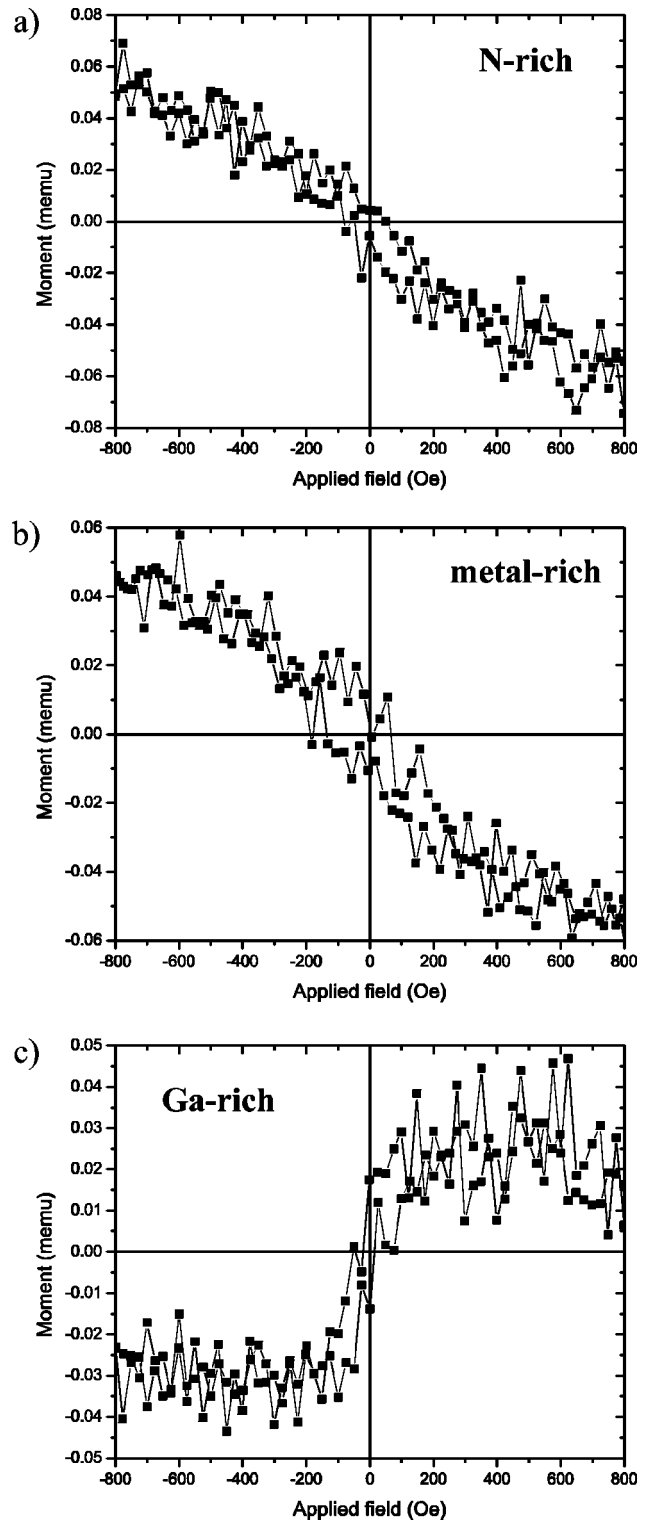


FIG. 7. VSM measurements of (a) N-rich grown film ($J_{\text{Ga}}/J_{\text{N}}=0.76$), (b) metal-rich grown film ($J_{\text{Ga}}/J_{\text{N}}=0.92$), and (c) Ga-rich grown film ($J_{\text{Ga}}/J_{\text{N}}=1.21$). The diamagnetic substrate background has already been subtracted from the original data.

growth leads to microscopic precipitation of Mn-rich regions. It is known that both GaMn and Mn_4N have FM behavior (ferro and ferri, respectively).^{26,27} Therefore, the small FM loop for this sample is attributed to such types of metallic precipitates.

Although we have not yet observed the FM behavior at room temperature in our MnGaN films in which the Mn is incorporated on the Ga sites, we have shown that by choosing the N-rich or metal-rich growth conditions, the FM behavior due to metallic precipitation is eliminated. This makes it possible to move to the next step of intentional doping. Thus, these results imply that FM behavior is possible since Mn has been proven to be incorporated into the film on Ga sites, an important step to achieving the FM MnGaN dilute magnetic semiconductor.

IV. SUMMARY

The growth of (Ga,Mn)N by rf N-plasma MBE under Ga-rich, metal-rich, and N-rich conditions has been investigated. RHEED shows a streaky dim pattern for Ga-rich growth, a bright spotty pattern for N-rich growth, and a partly streaky pattern for slightly metal-rich conditions. Ga-rich growth results in microscopic precipitation and chemical inhomogeneity, while N-rich growth results in more uniform incorporation without microscopic precipitation. For metal-rich growth, Mn is incorporated but excess metal precipitates. RBS has shown that slightly metal-rich conditions result in Mn substituting for Ga at the level of $\sim 5\%$ in this study, and AFM confirms minimal precipitation. We also find that it is very difficult to determine the incorporation of Mn based on XRD analysis; negligible 0006 peak shifts are observed in our experience.

We have thus shown that either metal-rich or N-rich conditions are necessary for achieving substitutional Mn incorporation on the Ga sites. Metal-rich conditions result in films with better crystallinity compared with N-rich conditions, as determined by RBS channeling. This is presumed to be related to increased surface diffusion for the metal-rich case. Moreover, our AFM study finds that the smoothest surface morphologies occur for either Ga-rich conditions (not including the precipitates) or for slightly metal-rich conditions. Therefore, in order to provide both Mn incorporation on Ga sites and the smoothest surface morphology, it is concluded that the optimal growth conditions for Ga-polar MnGaN by rf N-plasma MBE are in the slightly metal-rich regime.

We also found that the Ga polarity is maintained for N-rich, slightly metal-rich, and Ga-rich conditions. However, for increasingly metal-rich conditions (but not Ga-rich), the polarity is flipped, resulting in N polarity. This is attributed to Mn building up and forming a Mn-rich surface layer which leads to the inversion.

Finally, we reemphasize that the slightly metal-rich growth regime occurs for a metal/N incident flux ratio less than one in our definition due to the fact that N-rich, metal-rich, and Ga-rich are surface properties. The surface concentration ratios depend on both the flux rates of metal and N atoms and also the sticking coefficients of metal and N atoms (which vary with the flux rates).

ACKNOWLEDGMENTS

This material is based upon work supported by the National Science Foundation under Grant No. 9983816. Acknowledgment is also made to the Donors of the American Chemical Society Petroleum Research Fund, for partial support of this research.

- ¹T. Dietl, H. Ohno, F. Matsukura, J. Cibert, and D. Ferrand, *Science* **287**, 1019 (2000).
- ²H. Yang, H. Al-Britthen, E. Trifan, D. C. Ingram, and A. R. Smith, *J. Appl. Phys.* **91**, 1053 (2002).
- ³B. K. Rao and P. Jena, *Phys. Rev. Lett.* **89**, 185504 (2002).
- ⁴E. Kulatov, H. Nakayama, H. Mariette, H. Ohta, and Y. A. Uspenski, *Phys. Rev. B* **66**, 045203 (2002).
- ⁵L. Kronik, M. Jain, and J. R. Chelikowsky, *Phys. Rev. B* **66**, 041203(R) (2002).
- ⁶S. Kuwabara, K. Ishii, S. Haneda, T. Kondo, and H. Munekata, *Physica E (Amsterdam)* **10**, 233 (2001).
- ⁷M. Zajac, J. Gosk, M. Kamińska, A. Twardowski, T. Szyszko, and S. Podsiadlo, *Appl. Phys. Lett.* **79**, 2432 (2001).
- ⁸M. Zajac, R. Doradziński, J. Gosk, J. Szczytko, M. Lefeld-Sosnowska, M. Kamińska, A. Twardowski, M. Palczewska, E. Grzanka, and W. Gębicki, *Appl. Phys. Lett.* **78**, 1276 (2001).
- ⁹S. Kuwabara, T. Kondo, T. Chikyow, P. Ahmet, and H. Munekata, *Jpn. J. Appl. Phys., Part 2* **40**, L724 (2001).
- ¹⁰M. E. Overberg, C. R. Abernathy, S. J. Pearton, N. A. Theodoropoulou, K. T. McCarthy, and A. F. Hebard, *Appl. Phys. Lett.* **79**, 1312 (2001).
- ¹¹G. T. Thaler, M. E. Overberg, B. Gila, R. Frazier, C. R. Abernathy, S. J. Pearton, J. S. Lee, S. Y. Lee, Y. D. Park, Z. G. Khim, J. Kim, and F. Ren, *Appl. Phys. Lett.* **80**, 3964 (2002).
- ¹²Y. Cui and L. Li, *Appl. Phys. Lett.* **80**, 4139 (2002).
- ¹³S. Sonoda, S. Shimizu, T. Sasaki, Y. Yamamoto, and H. Hori, *J. Cryst. Growth* **237**, 1358 (2002).
- ¹⁴S. Sonoda, H. Hori, Y. Yamamoto, T. Sasaki, M. Sato, S. Shimizu, K.-I. Suga, and K. Kindo, *IEEE Trans. Magn.* **38**, 2859 (2002).
- ¹⁵R. Held, D. E. Crawford, A. M. Johnson, A. M. Dabiran, and P. I. Cohen, *J. Electron. Mater.* **26**, 272 (1997); R. A. Held, G. Nowak, B. E. Ishaug, S. M. Seutter, A. Parkhomovsky, A. M. Dabiran, P. I. Cohen, I. Grzegory, and S. Porowski, *J. Appl. Phys.* **85**, 7697 (1999).
- ¹⁶E. J. Tarsa, B. Heying, X. H. Wu, P. Fini, S. P. DenBaars, and J. S. Speck, *J. Appl. Phys.* **82**, 5472 (1997).
- ¹⁷R. M. Feenstra, H. Chen, V. Ramachandran, C. D. Lee, A. R. Smith, J. E. Northrup, T. Zyweitz, J. Neugebauer, and D. W. Greve, *Surf. Rev. Lett.* **7**, 601 (2000).
- ¹⁸T. Zyweitz, J. Neugebauer, and M. Scheffler, *Appl. Phys. Lett.* **73**, 487 (1998).
- ¹⁹A. R. Smith, R. M. Feenstra, D. W. Greve, M.-S. Shin, M. Skowronski, J. Neugebauer, and J. E. Northrup, *Surf. Sci.* **423**, 70 (1999).
- ²⁰J. E. Northrup, J. Neugebauer, R. M. Feenstra, and A. R. Smith, *Phys. Rev. B* **61**, 9932 (2000).
- ²¹A. R. Smith, R. M. Feenstra, D. W. Greve, M.-S. Shin, M. Skowronski, J. Neugebauer, and J. E. Northrup, *Appl. Phys. Lett.* **72**, 2114 (1998).
- ²²V. Ramachandran, R. M. Feenstra, W. L. Sarney, L. Salamanca-Riba, J. E. Northrup, L. T. Romano, and D. W. Greve, *Appl. Phys. Lett.* **75**, 808 (1999).
- ²³L. R. Doolittle, *Nucl. Instrum. Methods Phys. Res. B* **9**, 334 (1985).
- ²⁴National Compound Semiconductor Roadmap, <http://ncsr.csci-va.com>
- ²⁵K. Sato and H. Katayama-Yoshida, *Semicond. Sci. Technol.* **17**, 367 (2002).
- ²⁶M. Tanaka, J. P. Harbison, T. Sands, B. Philips, T. L. Cheeks, J. De Boeck, L. T. Florez, and V. G. Keramidas, *Appl. Phys. Lett.* **63**, 696 (1993).
- ²⁷K.-M. Ching, W.-D. Chang, and T.-S. Chin, *Appl. Surf. Sci.* **92**, 471 (1996).